Chiral crossover transition in a finite volume*

Chao Shi(史潮)[1;1)] Wenbao Jia(贾文宝)[2;2)] An Sun(孙安)[1] Liping Zhang(张力平)[3] Hongshi Zong(宗红石)[1,4,5;3)]

[1] College of Engineering and Applied Sciences, Nanjing University, Nanjing 210093, China
[2] College of Materials Science and Engineering, Nanjing University of Aeronautics and Astronautics, Nanjing 210016, China
[3] Key laboratory of road construction & equipment of MOE, Chang'an University, Xi'an 710064, China
[4] Key Laboratory of Theoretical Physics, Institute of Theoretical Physics, CAS, Beijing 100190, China
[5] Joint Center for Particle, Nuclear Physics and Cosmology, Nanjing 210093, China

Abstract: Finite volume effects on the chiral crossover transition of strong interactions at finite temperature are studied by solving the quark gap equation within a cubic volume of finite size L. With the anti-periodic boundary condition, our calculation shows the chiral quark condensate, which characterizes the strength of dynamical chiral symmetry breaking, decreases as L decreases below 2.5 fm. We further study the finite volume effects on the pseudo-transition temperature T_c of the crossover, showing a significant decrease in T_c as L decreases below 3 fm.

Keywords: chiral crossover transition, finite-volume effects, quark gap equation

PACS: 12.38.Mh, 11.10.Wx, 64.60.an **DOI:** 10.1088/1674-1137/42/2/023101

1 Introduction

It is widely believed that the universe went through a quark epoch approximately 10^{-12} seconds after the Big Bang, when the quarks and gluons formed a quark-gluon plasma (QGP) state at extremely high temperature. Nowadays, heavy ion collisions (HICs) at CERN (France/Switzerland), BNL (USA), and GSI (Germany) can reproduce such a state in the laboratory [1, 2]. It is found that QGP consists of unbound quarks/gluons and behaves as a nearly perfect fluid with low viscosity [3, 4]. On the theory side, nonperturbative QCD methods such as lattice QCD and effective theories have identified color de-confinement and chiral symmetry restoration in QGP [5–7], along with its many thermodynamic properties, e.g., its equation of state and various response functions [8–10]. The interplay between HIC experiments and theoretical studies will help us understand the profound phase structure of strongly interacting matter.

However, it should be noted that in HICs the QGP system produced always has a finite size. Depending on the collision nuclei, the center of mass energy and the centrality, the volume of the system varies. For example, analysis based on the UrQMD transport approach [11] shows that the volume of homogeneity before freeze-out for Au-Au and Pb-Pb collisions ranges between approximately $50 \sim 250$ fm^3 [12]. There is also an estimation [13] that the volume of the smallest QGP system produced at RHIC could be as low as (2 fm)^3. Therein the authors argue that finite volume effects could be relevant in the context of HICs, i.e., smoothening those singularities and generating shifted peaks and pseudocritical observables, and the information in thermodynamic limit (infinite volume) of QCD may be extracted with the finite-size scaling (FSS).

Finite volume effects in the thermodynamics of strong interactions have therefore been the subject of extensive theoretical interest. Chiral perturbation theory has investigated the implications of finite system size in various aspects [14–16], including the shift of pion mass and chiral quark condensate. This problem is further discussed using the renormalization group methods in the framework of the quark-meson model [17, 18]. Therein the non-negligible finite volume corrections to the chiral phase diagram are also addressed. The PNJL model obtained similar results [19–21] and further studied the volume dependence in quark number and isospin number susceptibilities.

In this connection, we employ the Dyson-Schwinger equations (DSEs) formalism to study the QCD chiral crossover transition at finite temperature and finite volume by solving the quark gap equation. It is a suit-

Received 9 November 2017, Published online 5 January 2018

∗ Supported by National Natural Science Foundation of China (11475085, 11535005, 11690030, 51405027), the Fundamental Research Funds for the Central Universities (020414380074), China Postdoctoral Science Foundation (2016M591808) and Open Research Foundation of State Key Lab. of Digital Manufacturing Equipment & Technology in Huazhong University of Science & Technology (DMETKF2015015)

1) E-mail: shichao@chenwang.nju.edu.cn

2) E-mail: jiawb@nuaa.edu.cn

3) E-mail: zonghs@nju.edu.cn

able QCD-connected non-perturbative formalism since it takes the quarks and gluons as the fundamental degrees of freedom, with key features like color confinement and dynamical chiral symmetry breaking (DCSB) preserved. Numerous successes in hadron physics [22] and the QCD phase diagram [23, 24] have been achieved, including the aforementioned finite volume effects on the shift of pion mass and chiral condensate [25], but those studies were all for zero temperature. In this work, we will generalize the DSEs study to both finite temperature and finite size.

Recently, the importance of choosing the proper boundary conditions in finite volume effect studies has been re-emphasized in Ref. [26]. We want to point out that consistent results from the aforementioned model studies are *all* obtained based on a specific boundary condition, which requires the fields to take the same boundary condition in their spatial and temporal directions. We will explain this in detail in the next section.

This paper is organized as follows. In Section 2 we introduce the quark gap equation at finite temperature and finite volume. The spatial boundary conditions will be discussed. Then in Section 3 we study the volume effects on the transition behavior of QCD at finite temperature by calculating the quark chiral condensate and chiral susceptibility. Finally we summarize our results and give conclusions in Section 4.

2 Quark gap equation in a finite volume

The quark gap equation, namely the Dyson-Schwinger equation for the quark propagator, is a non-perturbative equation essentially describing the motion of a two-point quark Green's function. The quark gap equation at finite temperature in an infinite volume reads

$$[G(\vec{p},\omega_n)]^{-1} = [G^0(\vec{p},\omega_n)]^{-1}+T\sum_{l=-\infty}^{\infty}\int\frac{\mathrm{d}^3q}{(2\pi)^3} \times\left[g^2D_{\mu\nu}(\vec{p}-\vec{q},\omega_n-\omega_l)\frac{\lambda^a}{2}\gamma_\mu G(\vec{q},\omega_l)\Gamma^a_\nu\right], \tag{1}$$

where $G(\vec{p},\omega_n)$ is the fully dressed quark propagator at finite temperature and $G^0(\vec{p},\omega_n)$ is the free one. The quark's Matsubara frequency is $\{\omega_n{=}n\pi T,\ n=\pm1,\pm3,...\}$, satisfying the anti-periodic boundary conditions for a fermion field in the temporal direction. From Eq. (1), the gluon's Matsubara frequency is $\{\Omega_n{=}n\pi T,\ n=0,\pm2,...\}$, so the periodic boundary conditions for the boson field are naturally satisfied. Since we will use gluon models that are heavily suppressed in the ultraviolet region, the integral/summation on the right-hand side of Eq. (1) is convergent and therefore no renormalization procedure is needed. The quark propagator at finite temperature can generally be decomposed as [27]

$$G^{-1}(\vec{p},\omega_n;T) = i\vec{\gamma}\cdot\vec{p}A(\vec{p}^{\,2},\omega_n;T)+\mathbb{I}_4B(\vec{p}^{\,2},\omega_n;T) +i\gamma_4\omega_nC(\vec{p}^{\,2},\omega_n;T), \tag{2}$$

where A,B and C are scalar functions. Note that for the free quark propagator $G^0(\vec{p},\omega_n)$, the scalar functions are $A=1,\ B=m$ and $C=1$, where m is the current quark mass.

At finite volume, e.g., a cubic box of volume L^3, the fields are constrained by spatial boundary conditions. However, unlike the thermal Matsubara frequencies, which are fixed by the statistics of the fields, there is no such restriction for the boundary conditions in the spatial directions. For the quark fields, popular boundary conditions include the periodic boundary condition (PBC) and anti-periodic boundary condition (APBC) [14]. For the PBC the momentum $\vec{p}$ takes discretized values as

$$\vec{p}_n=\sum_{n_i=0,\pm2,\pm4,...}n_i\pi/L\hat{e}_i, \tag{3}$$

while for the APBC

$$\vec{p}_n=\sum_{n_i=\pm1,\pm3,...}n_i\pi/L\hat{e}_i, \tag{4}$$

where $\hat{e}_i$ are the Cartesian unit vectors in Euclidean momentum space. The PBC tends to reduce the finite volume effect and surface effect, and hence is favored by lattice QCD simulations aiming for the thermodynamic limit. On the other hand, the APBC for quarks is widely employed in model studies, as introduced in the last section. The authors of Ref. [14] pointed out that in a practical effective model study, one should choose a specific boundary condition which requires the fields to take the same boundary condition in their spatial and temporal directions. In our case, the quark should take the APBC and the gluon should take the PBC. This has the powerful consequence that the partition function allows a permutation symmetry of the spatial and temporal directions, i.e., L and $\beta{=}1/T$. The symmetry carries over to the Lagrangian, rendering temperature- and volume- independent coupling constants. In this sense, we can directly generalize our study to finite volume without tuning the model parameters which were determined at infinite volume. We therefore employ the APBC for quarks (the gluons automatically take the PBC in Eq. (6)) throughout our calculations in this work.

Discretizing the momentum in Eq. (1) and using

$$\int\frac{\mathrm{d}p^3}{(2\pi)^3}(\cdots)\to\frac{1}{L^3}\sum_{n_j=-\infty}^{\infty}(\cdots), \tag{5}$$

the quark gap equation at finite temperature and finite volume can be obtained

$$[G(\vec{p}_{\mathbf{n}},\omega_n)]^{-1} = [G^0(\vec{p}_{\mathbf{n}},\omega_n)]^{-1}+\frac{T}{L^3}\sum_{l_j,l=-\infty}^{\infty}\left[g^2 D_{\mu\nu}(\vec{p_{\mathbf{n}}}-\vec{q}_{\mathbf{l}},\omega_n-\omega_l)\frac{\lambda^a}{2}\gamma_\mu G(\vec{q}_{\mathbf{l}},\omega_l)\Gamma^a_\nu\right]. \quad (6)$$

The quark propagator is then decomposed as

$$G^{-1}(\vec{p}_{\mathbf{n}},\omega_n;T) = i\vec{\gamma}\cdot\vec{p}_{\mathbf{n}}A(\vec{p}_{\mathbf{n}},\omega_n;T)+\mathbb{I}_4 B(\vec{p}_{\mathbf{n}},\omega_n;T) +i\gamma_4\omega_n C(\vec{p}_{\mathbf{n}},\omega_n;T). \quad (7)$$

There are several symmetries lying in these scalar functions $\mathcal{F} = A,\ B$ or C. Although there is no longer $O(3)$ symmetry in the spatial directions, there are still some left. For example, if we denote $\mathcal{F}(\vec{p}_{\mathbf{n}},\omega_n;T) = \mathcal{F}(n_1,n_2,n_3,\omega_n;T)$, then one could expect the reflection symmetry to hold, leading to

$$\mathcal{F}(n_1,n_2,n_3,\omega_n;T)=\mathcal{F}(\pm n_1,\pm n_2,\pm n_3,\omega_n;T). \quad (8)$$

Further, the scalar functions $\mathcal{F}$ are invariant under the permutation of n_1,n_2 and n_3

$$\mathcal{F}(n_1,n_2,n_3,\omega_n;T)=\mathcal{F}(\{n_1,n_2,n_3\},\omega_n;T), \quad (9)$$

where $\{n_1,n_2,n_3\}$ is any possible permutation of n_1,n_2 and n_3. We also have in the temporal direction that $\omega_n\to\omega_{-n}$ brings $\mathcal{F}$ to its complex conjugate [27],

$$\mathcal{F}(n_1,n_2,n_3,\omega_n;T)=\mathcal{F}^*(n_1,n_2,n_3,\omega_{-n};T). \quad (10)$$

We will show later that these relations allow a large reduction of the independent $\mathcal{F}(n_1,n_2,n_3,\omega_n;T)$ space, greatly optimizing the numerical computation.

To solve the quark gap equation Eq. (1) or Eq. (6), truncations are indispensable. Here we follow Ref. [10] and employ the Rainbow truncation

$$\Gamma^a_\nu(p,q)=\frac{\lambda^a}{2}\gamma_\nu. \quad (11)$$

Despite it being a great simplification, as far as we know there is no improvement to Eq. (11) that gives any qualitatively different results concerning the chiral phase transition. We also employ the gluon propagator model known as the Maris-Tandy model [28], which has achieved great success in hadron physics,

$$g^2 D_{\mu\nu}(Q^2)=\frac{4\pi^2}{\omega^6}De^{-Q^2/\omega^2}(Q^2\delta_{\mu\nu}-Q_\mu Q_\nu). \quad (12)$$

In Ref. [10], we sketched the QCD phase diagram with this model using the preferred parameters ω=0.45 GeV and $D\omega = (0.8\ \text{GeV})^3$. As is apparent in Eq. (12), we choose the Landau gauge, which is a fixed point of the renormalization group. It gives less sensitivity to model-dependent differences between Ansatze for the fermion-gauge boson vertex, and hence is widely used in Dyson-Schwinger equation studies.

3 Finite volume effects on QCD chiral diagram at finite temperature

In this section, we discuss the chiral phase diagram at finite temperature and finite volume. Especially, we will investigate the quark chiral condensate, which is the order parameter of chiral symmetry restoration in the chiral limit (m=0) and a good indicator of DCSB beyond the chiral limit ($m\neq 0$). The crossover behavior, along with the pseudo-transition temperature and volume dependence, will be shown.

We first solve the quark gap equations. At infinite volume, the solution to Eq. (1) with model Eq. (12) has been presented in Ref. [10], where the details can be found. Here, we focus on Eq. (6) at finite volume. The procedure is to insert Eqs. (7, 11, 12) into Eq. (6), multiply each side by $-i\vec{p}_n\cdot\vec{\gamma}$, $\mathbb{I}_4$ and $-i\omega_l\gamma_4$ respectively, and then take traces on both sides. We have abbreviated $p_n = (p_{n_1},p_{n_2},p_{n_3},\omega_n) \equiv (\vec{p}_n,\ \omega_n)$ and $q_l = (q_{l_1},q_{l_2},q_{l_3},\omega_l) \equiv (\vec{q}_l,\ \omega_l)$. For the scalar functions, $\mathcal{F}(\vec{p}_n,\omega_n;T) = \mathcal{F}_p$ and $\mathcal{F}(\vec{q}_l,\omega_l;T) = \mathcal{F}_q$. The following coupled non-linear equations can then be obtained:

$$\vec{p}_n^2 A_p=\vec{p}_n^2+\sum_{l_i,l=-\infty}^{\infty}\mathcal{C}(T,n,l)\frac{A_q(\vec{p}_n\cdot\vec{q}_l[(p_n-q_l)^2+2(\vec{p}_n-\vec{q}_l)^2]-2(\vec{p}_n\times\vec{q}_l)^2)+2C_q[(\vec{p}_n-\vec{q}_l)^2+\vec{p}_n\cdot\vec{q}_l]}{A_q^2\vec{q}_l^2+B_q^2+C_q^2\omega_l^2}, \quad (13)$$

$$B_p=m+\sum_{l_i,l=-\infty}^{\infty}\mathcal{C}(T,n,l)\frac{3B_q(p_n-q_l)^2}{A_q^2\vec{q}_l^2+B_q^2+C_q^2\omega_l^2}, \quad (14)$$

$$\omega_n^2 C_p=\omega_n^2+\sum_{l_i,l=-\infty}^{\infty}\mathcal{C}(T,n,l)\frac{2A_q(\vec{p}_n\cdot\vec{q}_l-\vec{q}_l^2)\omega_n(\omega_n-\omega_l)+C_q\omega_n\omega_l[(p_n-q_l)^2+2(\omega_n-\omega_l)^2]}{A_q^2\vec{q}_l^{\,2}+B_q^2+C_q^2\omega_l^2}, \quad (15)$$

$$\mathcal{C}(T,n,l)=\frac{4}{3}\frac{T}{L^3}\frac{4\pi^2}{\omega^6}De^{-(p_n-q_l)^2/\omega^2}. \quad (16)$$

These coupled non-linear equations can be numerically solved by iteration. As mentioned in last section, regarding Eqs. (8,9,10) the number of truly independent $\mathcal{F}(n_1,n_2,n_3,\omega_n)$ is much less than naively expected. For example, in a practical computation the typical choice is for n_i and n to vary between around $[-15,15]$. This would require about 200,000 $\mathcal{F}(n_1,n_2,n_3,\omega_n)$'s for iteration, while one can reduce the number to about 10,000 using Eqs. (8)–(10), rendering the computation practicable.

Now we can look at the chiral quark condensate $\langle\bar{\psi}\psi\rangle$ which characterizes the DCSB. Using the fully dressed quark propagator, it can be calculated as [24]

$$-\langle\bar{\psi}\psi\rangle_L = N_c N_f \frac{T}{L^3} \sum_{n_i,n=-\infty}^{\infty} \mathrm{Tr}[G(\vec{p}_n,\omega_n;T) - G_0(\vec{p}_n,\omega_n;T)]. \tag{17}$$

The $-\langle\bar{\psi}\psi\rangle_L$'s at different L's are plotted in Fig. 1, with a few things noticeable. Firstly, when $L \geqslant 3$ fm, $-\langle\bar{\psi}\psi\rangle_L$ is indistinguishable from that at $L=\infty$. This is natural since the finite volume effects should gradually diminish as the volume increases and finally approaches the thermodynamic limit. The quark meson model [18] also found that when the pion mass $m_\pi \geqslant 200$ MeV, the results approach the infinite volume limit as $L \geqslant 3$ fm. However, this is only at finite temperature. If a finite chemical potential is introduced, the QCD $T-\mu$ phase diagram, especially the location of the critical end point (CEP), would approach the thermodynamic limit at larger L, as exemplified in Ref. [17]. Since the size of the HIC created fireball could go as low as $(2\ \mathrm{fm})^3$, these calculations could be relevant. Secondly, $-\langle\bar{\psi}\psi\rangle_L$ generally decreases as L decreases below 2.5 fm. This behavior is consistent with early findings. For example, the authors of Ref. [25] studied the quark gap equation at finite volume with zero temperature. They found the dynamical quark mass generation rises rapidly until it reaches a plateau at $L=2$ fm. In particular, this behavior is qualitatively consistent with lattice QCD computations in the case of $N_f=3$ and $N_f=2+1$ at finite temperature [30, 31]. Note that in lattice QCD the PBC for is commonly employed for the quark field . In our case, this behavior can be easily understood if one realizes that the APBC allows the permutation symmetry of L and $\beta=1/T$ in the partition function. Therefore $-\langle\bar{\psi}\psi\rangle_L$ should have the same monotonicity for L and β, namely, $-\langle\bar{\psi}\psi\rangle_L$ decreases as L decreases and/or T increases.

We further look at the chiral susceptibility

$$\chi_L^m(T) = -\frac{\partial}{\partial m}\langle\bar{\psi}\psi\rangle_L \tag{18}$$

to study the crossover behavior at finite temperature and finite volume. The size dependence are plotted in Fig. 2. We denote the maximum of these curves as the pseudo-critical temperature T_c. While the definition of T_c with respect to different susceptibilities brings ambiguities, the values of the T_c's will not differ much. Especially, the shift of T_c's in L will not be qualitatively altered. When approaching the thermodynamic limit we have $T_c=165$ MeV, close to the lattice QCD simulation value $T_c=154(9)$ MeV [29]. There is then a sizable decrease in T_c from 165 MeV to 120 MeV while the system size decreases from 3 fm to 1.8 fm, as listed in Table 1. This result is also consistent with the quark-meson model study [18]. In this connection, we think the finite volume effects could be non-negligible for the small QGP systems created in peripheral collisions.

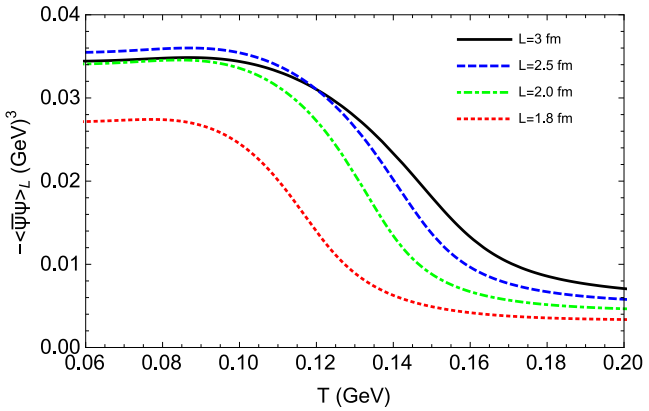

Fig. 1. (color online) The chiral quark condensate $-\langle\bar{\psi}\psi\rangle_L$ at different volumes. The black solid line displays the result at $L=3.0$ fm, with the dashed (blue), dot-dashed (green), and dotted (red) lines corresponding to $L=2.5$, 2.0, 1.8 fm respectively. The curve for $L=\infty$ is indistinguishable from $L=3$ fm and hence not plotted.

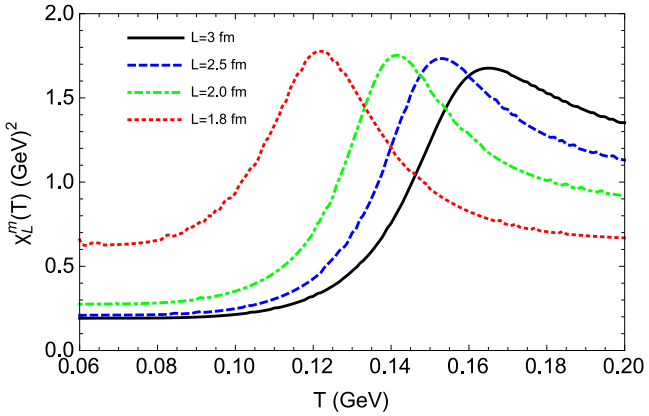

Fig. 2. (color online) The chiral susceptibility $\chi_L^m(T)$ at different volumes. The black solid line displays the result at $L=3.0$ fm, with the dashed (blue), dot-dashed (green), and dotted (red) lines corresponding to $L=2.5$, 2.0, 1.8 fm respectively. The curve for $L=\infty$ is indistinguishable from $L=3$ fm and hence not plotted.

Table 1. Pseudo-critical temperature T_c at different sizes L.

L/fm	1.8	2.0	2.2	3.0
T_c/MeV	122	141	153	165

4 Summary

Based on the QCD-connected DSEs formalism, we have investigated the finite volume effects on the chiral crossover transition of QCD at finite temperature by solving the quark gap equation in a cubic volume of finite size L. The merit of the quark's anti-periodic boundary condition is highlighted. Our calculation shows the chiral quark condensate decreases as L decreases below 2.5 fm. This is understood with the permutation symmetry of L and $\beta=1/T$ in the partition function. We further studied the finite volume effects on the pseudo-critical temperature T_c of the crossover, showing a decrease in T_c as L decreases. The qualitative behavior is in agreement with existing model studies [17, 18, 25] and lattice QCD computations [30, 31]. Our results therefore imply that finite volume effects could be non-negligible for peripheral collisions in HICs. The theoretical framework and techniques we developed can readily be applied to more complicated situations such as studying the whole $T-\mu$ QCD phase diagram.

References

1 J. Adams et al (STAR Collaboration), Nucl. Phys. A, **757**: 102 (2005)
2 E. Shuryak, Prog. Part. Nucl. Phys., **62**: 48 (2009)
3 E. Shuryak, Prog. Part. Nucl. Phys., **53**: 273 (2004)
4 W. A. Zajc, Nucl. Phys. A, **805**: 283 (2008)
5 E. Bilgici, F. Bruckmann, C. Gattringer, and C. Hagen, Phys. Rev. D, **77**: 094007 (2008)
6 C. S. Fischer, Phys. Rev. Lett., **103**: 052003 (2009)
7 G. Endrodi, Z. Fodor, S. D. Katz, and K. K. Szabo, JHEP, **1104**: 001 (2011)
8 M. Asakawa and K. Yazaki, Nucl. Phys. A, **504**: 668 (1989)
9 A. Bazavov et al (HotQCD Collaboration), Phys. Rev. D, **90**: 094503 (2014)
10 C. Shi, Y. L. Wang, Y. Jiang, Z. F. Cui, and H. S. Zong, JHEP, **1407**: 014 (2014)
11 S. A. Bass et al, Prog. Part. Nucl. Phys., **41**: 255 (1998)
12 G. Graef, M. Bleicher, and Q. Li, Phys. Rev. C, **85**: 044901 (2012)
13 L. F. Palhares, E. S. Fraga, and T. Kodama, J. Phys. G, **38**: 085101 (2011)
14 J. Gasser and H. Leutwyler, Phys. Lett. B, **188**: 477 (1987)
15 F. C. Hansen, Nucl. Phys. B, **345**: 685 (1990).
16 P. H. Damgaard and H. Fukaya, JHEP, **0901**: 052 (2009)
17 J. Braun, B. Klein, and B. J. Schaefer, Phys. Lett. B, **713**: 216 (2012)
18 J. Braun, B. Klein, H.-J. Pirner, and A. H. Rezaeian, Phys. Rev. D, **73**: 074010 (2006)
19 A. Bhattacharyya, R. Ray, and S. Sur, Phys. Rev. D, **91**(5): 051501 (2015)
20 A. Bhattacharyya, P. Deb, S. K. Ghosh, R. Ray, and S. Sur, Phys. Rev. D, **87**(5): 054009 (2013)
21 Z. Pan, Z. F. Cui, C. H. Chang, and H. S. Zong, Int. J. Mod. Phys. A, **32**(13): 1750067 (2017)
22 C. D. Roberts, Prog. Part. Nucl. Phys., **61**: 50 (2008)
23 C. S. Fischer and J. Luecker, Phys. Lett. B, **718**: 1036 (2013)
24 C. Shi, Y. L. Du, S. S. Xu, X. J. Liu, and H. S. Zong, Phys. Rev. D, **93**(3): 036006 (2016)
25 J. Luecker, C. S. Fischer, and R. Williams, Phys. Rev. D, **81**: 094005 (2010)
26 B. Klein, Phys. Rept., **09**: 002 (2017)
27 C. D. Roberts and S. M. Schmidt, Prog. Part. Nucl. Phys., **45**: S1 (2000)
28 P. Maris and P. C. Tandy, Phys. Rev. C, **60**: 055214 (1999)
29 A. Bazavov *et al.*: Phys. Rev. D **85**: 054503 (2012)
30 H.-T. Ding, A. Bazavov, F. Karsch, Y. Maezawa, S. Mukherjee, and P. Petreczky, PoS LATTICE, **2013**: 157 (2014)
31 A. Bazavov, H.-T. Ding, P. Hegde, F. Karsch, E. Laermann, S. Mukherjee, P. Petreczky, and C. Schmidt, Phys. Rev. D, **95**(7): 074505 (2017)